

Potential impact of WTAP and YTHDF2 on tumor immunity in lung adenocarcinoma

Xinyu Zhang, PhD^a, Xinsheng Cai, PhD^{b,*}

Abstract

WTAP and N6-methyladenosine (m6A) reader proteins (YTHDF2) are N6-methyladenosine (m6A) methyltransferase and m6A reading proteins, respectively. In recent years, the tumor immune environment has received more and more attention in the progress and treatment of cancer. The aim of this study was to investigate the relationship between N6-methyladenosine (m6A) methyltransferase (WTAP)/YTHDF2 and the immunological characteristics of lung adenocarcinoma (LUAD). Based on the expression of WTAP and YTHDF2 in the cancer genome atlas (TCGA) and gene expression omnibus (GEO) database, LUAD patients were divided into 2 clusters by coherently clustering method, and performed gene set enrichment analysis (GSEA) to identify the functional differences. Immunoinvasion analysis was performed using ESTIMATE, CIBERSORT, and single-sample GSEA (ssGSEA), and expression of immune checkpoint inhibitors (ICIs) targets was assessed, while tumor mutation burden (TMB) was calculated in tumor samples. Weighted gene co-expression network analysis (WGCNA) was used to identify the genes related to both WTAP/YTHDF2 expression and immunity. The immunological characteristics between the 2 clusters were externally verified based on GSE39582. The expression of WTAP was higher in cluster 1 and YTHDF2 was lower, but it was opposite in cluster 2. Cluster 1 had stronger immune infiltration, more ICIs target expression, more TMB. In addition, WGCNA identified 22 genes associated with WTAP/YTHDF2 expression and immune score, including TIM3 (HAVCR2) and CD86. WTAP and YTHDF2 influence immune contexture and may be novel prognostic and druggable targets associated with the immune system of LUAD.

Abbreviations: GEO = gene expression omnibus, GO = gene ontology, GSEA = gene set enrichment analysis, ICIs = immune checkpoint inhibitors, LUAD = lung adenocarcinoma, m6A = N6-methyladenosine, NSCLC = non-small cell lung cancer, POLE = polymerase epsilon, ssGSEA = single-sample GSEA, TCGA = the cancer genome atlas, TMB = tumor mutation burden, WGCNA = weighted gene co-expression network analysis, WTAP = N6-methyladenosine (m6A) methyltransferase, YTHDF2 = N6-methyladenosine (m6A) reader proteins.

Keywords: immune environment, lung adenocarcinoma, m6A, WTAP, YTHDF2

1. Introduction

Lung cancer is the second most common cancer in the world in 2020 and the leading cause of cancer deaths in 2020.^[1] Lung adenocarcinoma (LUAD) is the most common subtype, accounting for about 40% of lung cancer. LUAD patients are usually diagnosed at late stages of the disease.^[2] Despite advances in molecular diagnostics, targeted therapies and immunotherapy, the average 5-year survival rate for LUAD is still as low as 15%.^[3,4]

Immune checkpoint inhibitors (ICIs), particularly PD-1 inhibitors, have transformed the treatment of non-small cell lung cancer (NSCLC) in the last decade. However, PD-L1 and tumor mutational burden (TMB) have not been shown to be direct indicative biomarkers for immunotherapy.^[5] Therefore, it is important to identify new immunotherapeutic markers and reveal the underlying mechanisms of immune checkpoints.

N6-methyladenosine (m6A) is the most abundant RNA modification in both coding and non-coding RNAs and is a critical post-transcriptional regulator in various cancers.^[6-8] Proteins involved in m6A modification can be divided into 3 categories: m6A methyltransferases (catalyzing the occurrence of m6A modification), m6A demethylases (catalyzing the removal of m6A modification) and m6A reading proteins (recognizing and binding m6A modification).^[9] While the intrinsic oncogenic processes of tumors are critical, the tumor and immune effects of m6A modifications are also of interest. In recent years, several studies have shown that targeting dysregulated m6A regulators with small molecule inhibitors has potential for cancer treatment. Considering the functional importance of m6A modifications in various cancers, targeting m6A modulators may be clinically applicable in combination with chemotherapy or immunotherapy to improve cancer treatment.^[10]

The authors disclosed receipt of the following financial support for the research, authorship, and/or publication of this article: This work was supported by Shandong Medical and Health Science and Technology Development Plan (grant number 2018WS068).

The authors have no conflicts of interest to disclose.

The datasets generated during and/or analyzed during the current study are publicly available.

The original contributions presented in the study are included in the article. Further inquiries can be directed to the corresponding authors.

Studies involving human participants have been reviewed and approved by the Institutional Ethics Committee of Weifang Hospital of Traditional Chinese Medicine. The patient/participant provided written informed consent to participate in the study.

^a Shandong University of Traditional Chinese Medicine, Jinan, China, ^b Weifang Hospital of Traditional Chinese Medicine, Weifang, China.

* Correspondence: Xinsheng Cai, Weifang Hospital of Traditional Chinese Medicine, Jinan 261000, China (e-mail: relative2000@126.com).

Copyright © 2022 the Author(s). Published by Wolters Kluwer Health, Inc. This is an open-access article distributed under the terms of the Creative Commons Attribution-Non Commercial License 4.0 (CCBY-NC), where it is permissible to download, share, remix, transform, and build upon the work provided it is properly cited. The work cannot be used commercially without permission from the journal.

How to cite this article: Zhang X, Cai X. Potential impact of WTAP and YTHDF2 on tumor immunity in lung adenocarcinoma. *Medicine* 2022;101:45(e31195).

Received: 19 July 2022 / Received in final form: 8 September 2022 / Accepted: 15 September 2022

<http://dx.doi.org/10.1097/MD.00000000000031195>

WTAP is an m6A methyltransferase. In hepatocellular carcinoma, N6-methyladenosine (m6A) methyltransferase (WTAP) can promote hepatocellular carcinoma progression through m6A-HuR-dependent epigenetic silencing of ETS1.^[11] Meanwhile, WTAP has been shown to affect tumor prognosis through tumor-associated T lymphocyte infiltration.^[12] N6-methyladenosine (m6A) reader proteins (YTHDF2) is an m6A reading protein, and YTHDF2 can play a role in mRNA stability and translation, and can mediate RNA decay.^[13] YTHDF2 promotes NK cell effector function and promotes IL-15-mediated NK cell survival and proliferation by forming a STAT5-YTHDF2 positive feedback loop, and YTHDF2 deficiency impairs NK cell anti-tumor capacity.^[14] Meanwhile, high expression of YTHDF2 leads to downregulation of PD-L1, which in turn affects the effectiveness of immunotherapy.^[15]

2. Materials and methods

2.1. Data sources and preprocessing

The cancer genome atlas (TCGA)-LUAD transcriptome analysis data (HTSeq-Counts and HTSeq-FPKM) were downloaded using the UCSC Xena website. HTSeq-FPKM data from 510 primary solid tumor specimens were transformed using $\log_2(\text{FPKM} + 1)$ and differential analysis was performed using HTSeq-Counts.

Collection of simple nucleotide variant data (mutect) from LUAD patients using the R package maftools.^[16] Due to the lack of information on mutations in some LUAD patients, we included only 460 patients in the analysis involving the mutation landscape. Based on the R software ComplexHeatmap package,

waterfall plots were used to show patients' mutations.^[17] Tumor mutational burden (TMB) was calculated based on simple nucleotide variants, defined as the number of mutations per megabase.

Expression profiling by GSE68465 array was downloaded from the Gene Expression Omnibus (GEO) database (<https://www.ncbi.nlm.nih.gov/gds/>).^[18] Validation of immune characteristics of LUAD patients using a dataset of 422 LUAD tissues.

2.2. Immuno-infiltration analysis

ESTIMATE is a method to identify stromal and immune cells based on gene expression profiles in tumor samples. It assesses the tumor microenvironment TME of LUAD patients by 4 dimensions: Stromal score, Immune score, ESTIMATE score and Tumor purity.^[19]

CIBERSORT is a method for calculating the composition of immune cells based on gene expression profiles.^[20] The algorithm calculates the proportion of 22 immune cells in LUAD patients. The sum of the 22 immune cell type fractions in each sample is 1.

The single sample gene set enrichment analysis (ssGSEA) method of R package GSVA^[21] was applied to calculate the degree of infiltration of 28 immune cell types.

2.3. Consensus clustering based on WTAP and YTHDF2

WTAP and YTHDF2 expressions were extracted and coherently clustered using the R package ConsensusClusterPlus.^[22] The samples were also divided into 2 clusters.

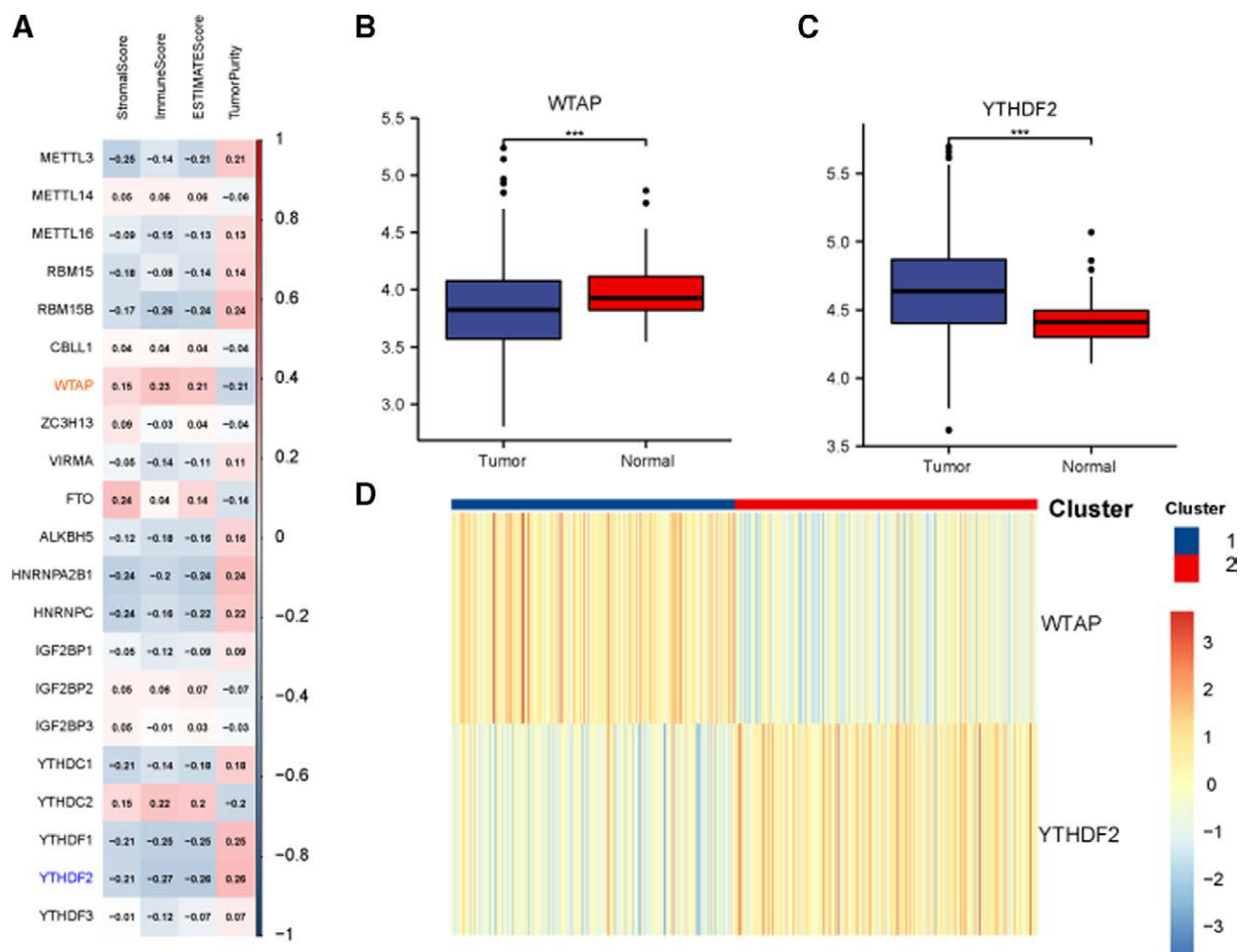


Figure 1. Identification of m6A regulators related to immune score and clustering of TCGA-LUAD patients based on WTAP and YTHDF2. (A) Association between m6A regulators and normal tissues. (C) TCGA-LUAD patients are divided into 2 clusters according to WTAP and YTHDF2. LUAD = lung adenocarcinoma, m6A = N6-methyladenosine, TCGA = the cancer genome atlas, WTAP = N6-methyladenosine (m6A) methyltransferase, YTHDF2 = N6-methyladenosine (m6A) reader proteins.

2.4. Gene set enrichment analysis

Based on the R package clusterProfiler^[23] performs GSEA to find significant functional differences between the 2 clusters. Significant pathway enrichment was identified by the *P* value < 0.05, normalized enrichment score |NES| >1, and FDR *q* value < 0.05.

2.5. Differential expressed genes

Differentially expressed genes in both clusters were identified by (HTSeq-Counts) data using the R package DESeq2.^[24] The threshold value was log2FoldChange >1 and FDR *q* value < 0.05.

2.6. Weighted gene co-expression network analysis (WGCNA)

We performed WGCNA on differential genes using the R package WGCNA.^[25] To ensure that the constructed co-expression network was close to a scale-free distribution, 3 was chosen as a soft threshold. A total of 20 modules were obtained and correlations of modules with stromal score, immune score, ESTIMATE score and tumor purity were calculated. Then, 22 genes were obtained based on module membership and gene significance calculations.

2.7. Functional enrichment analysis

Gene ontology (GO) analysis was performed using the R package clusterProfiler^[23] to analyze the functions of 22 differential genes. A protein-protein interaction network was constructed using the String database. Correlation between genes, correlation between genes and ESTIMATE, and correlation between genes and ssGSEA were analyzed using the R package corrrplot.

2.8. Specimen collection and Real-time quantitative Polymerase Chain Reaction (RT-qPCR)

Nine pairs of LUAD organizations and their adjacent organizations were collected from Weifang Hospital of Traditional Chinese Medicine and obtained informed consent and approval from the Ethics Committee of Weifang Hospital of Traditional Chinese Medicine.

Total RNA was extracted using TRIzol reagent (Invitrogen). cDNA was synthesized using PrimeScript RT Reagent Kit (TaKaRa). Real-time quantitative Polymerase Chain Reaction was performed using SYBR Prime Script RT-PCR kit (TaKaRa) according to the manufacturer’s protocol.

The primer sequences were as follows: WTAP-F 5’- GCTTCTGCCTGGAGAGGATT-3’; WTAP-R 5’- GTCTGTTTCACTCAATCGAACCT-3’; YTHDF2-F 5’- AGCCTCTTGGAGCAGTACAAA-3’; YTHDF2-R 5’-TGCATTATTGGGCCTTGCCT-3’; GAPDH-F 5’- GAAAGCCTGCCGGTGAATA-3’; GAPDH-R 5’- AGGAAAAGCATCACCCGGAG-3’.

2.9. Statistical analysis

Statistical analysis was performed based on R (4.1.2) and SPSS (21.0). Box plot analysis was performed using Wilcoxon rank sum test. Correlation analysis was performed using Spearman’s correlation analysis. Images were stitched by Adobe Illustrator (2021).

3. Results

3.1. Identification and consensus clustering of patients of immune-related m6a regulators

First, 4 ESTIMATE indices were calculated for each sample to assess the ratio of stromal cells to immune cells. To explore

the role of m6A modifications in tumor immunity of LUAD patients, 21 m6A regulators were identified and the correlation between m6A regulator expression and ESTIMATE results was assessed (Fig. 1A). WTAP and YTHDF2 had the highest correlation with the absolute value of immune score, so WTAP and YTHDF2 were included in the subsequent analysis. Wilcoxon rank sum test was performed for tumor tissues versus normal tissues using transcriptomic data from TCGA-LUAD; WTAP and YTHDF2 were differentially expressed in both tumor and normal tissues (Fig. 1B and C). Subsequently, a consensus clustering analysis was performed on 510 TCGA-LUAD samples based on the expression matrix of WTAP and YTHDF2. The samples were divided into 2 clusters (Fig. 1D). The heat map shows that cluster 1 (n = 247) was high expression of WTAP and low expression of YTHDF2; cluster 2 (n = 263) was high expression of YTHDF2 and low expression of WTAP.

3.2. Evaluation of clinical characteristics

To determine the differences in clinical characteristics between the 2 clusters, we first drew survival curves and found no significant differences in prognosis between the 2 clusters. Correlation analysis showed no significant differences in gender, age, TNM stage, and pathological stage between cluster 1 than cluster 2 (Table 1).

3.3. Identification of immune-related pathways by GSEA

All differentially expressed genes in cluster 1 and cluster 2 are contained in GSEA. We identified many important immune-related pathways in the enriched MSigDB Collection (c5.cp.v7.0.symbols.gmt), including adaptive immune response, cell chemotaxis, cytokine mediated signaling pathway, cytokine production, external_side of plasma membrane, G protein coupled receptor signaling pathway, humoral immune response, inflammatory response, innate immune response and leukocyte chemotaxis (Fig. 2A).

Table 1
Clinical features of two clusters.

	Cluster1	Cluster2	P value
Number	247	263	.553
Age	66[58.25,72.75]	67[59,73]	
Gender			.971
Female	126	149	
Male	121	114	
T stage			.797
T1	79	88	
T2	133	143	
T3	25	20	
T4	9	10	
TX	1	2	
N stage			.514
N0	161	166	
N1	43	52	
N2	38	36	
N3	2	0	
NX	3	9	
M stage			.792
M0	174	169	
M1	12	13	
MX	61	81	
Pathological stage			.912
Stage I	128	145	
Stage II	57	63	
Stage III	43	41	
Stage IV	13	13	
Not reported	6	1	

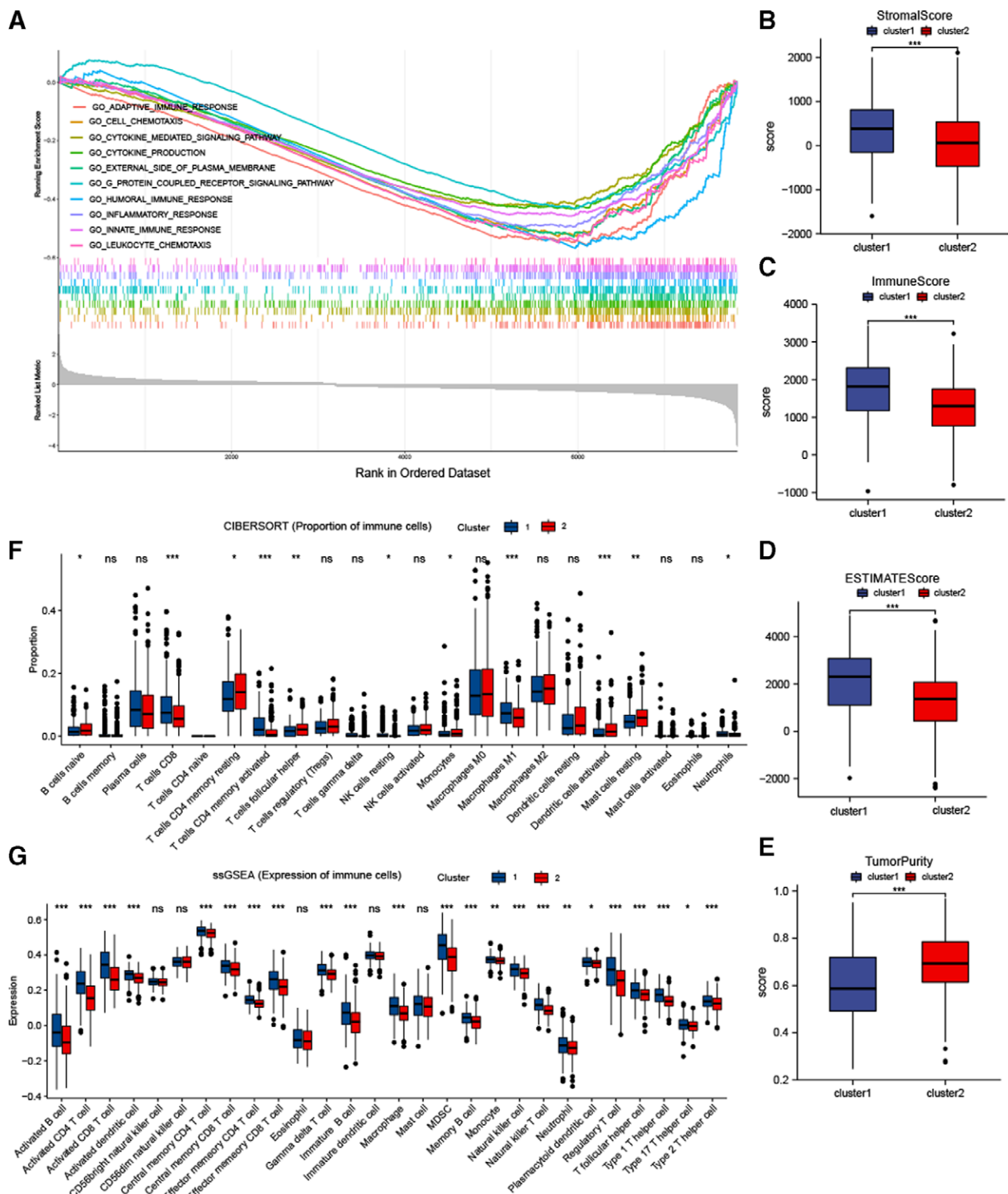


Figure 2. Comparison of immune characteristics between 2 clusters. Comparison of functional enrichment (A), stromal score (B), immune score (C), ESTIMATE score (D), tumor purity (E), proportion of immune cells (F) and expression of immune cells (G) between 2 clusters. The *P* values are labeled using asterisks (ns, no significance, **P* < .05, ***P* < .01, ****P* < .001).

3.4. Comparison of immune infiltration

Differences in immune function were calculated based on ESTIMATE, CIBERSORT and ssGSEA algorithms. In the ESTIMATE analysis, cluster 1 had higher stromal, immune and ESTIMATE scores and lower tumor purity compared to cluster 2 (Fig. 2B–E). In addition, CIBERSORT analysis showed that cluster 1 had a higher proportion of CD8 T cells (Fig. 2F). ssGSEA showed that 25 immune cell subtypes (e.g., activated B cells, activated CD4

T cells, activated CD8 T cells, activated dendritic cells, natural killer cells, and natural killer T cells) were highly expressed in cluster 1 (Fig. 2G). The results indicated that cluster 1 had stronger immune infiltration than cluster 2, especially in terms of CD8 T cells.

3.5. Immunotherapy sensitivity assessment

To assess the sensitivity of 2 clusters of LUAD patients to immunotherapy, we compared the expression of common

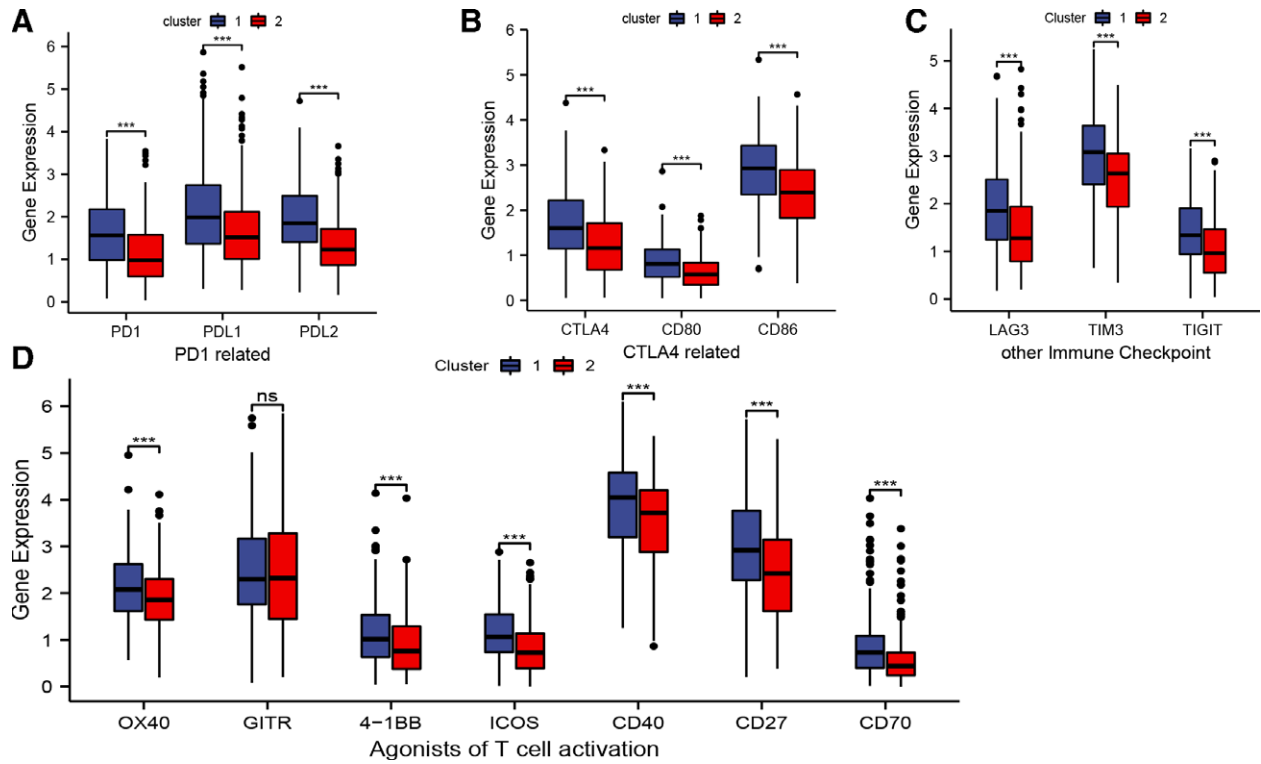


Figure 3. Comparison of immunomodulatory drugs' targets in clinical trials between 2 clusters. The *P* values are labeled using asterisks (****P* < .001).

immunomodulatory targets between the 2 clusters and found that most immunomodulatory targets (PD1, PDL1, PDL2, CTLA4, CD80, CD86, LAG3, TIM3, TIGIT, OX40, GITR, 4-1BB, ICOS, CD27, CD70) were significantly higher in expression in cluster 1 (Fig. 3A–D). The results suggest that cluster 1 may have a better response to immunotherapy than cluster 2.

3.6. Comparison of gene mutations

Different mutations have different effects on immunotherapy efficacy, so we evaluated the mutation status of LUAD patients and plotted the mutational landscape between the 2 clusters (Fig. 4A and B). Cluster 1 had a higher TMB and a higher number of MLH1, MSH2, MSH6, PMS2, polymerase epsilon (POLE) and POLD1 mutations than cluster 2 (Fig. 4C

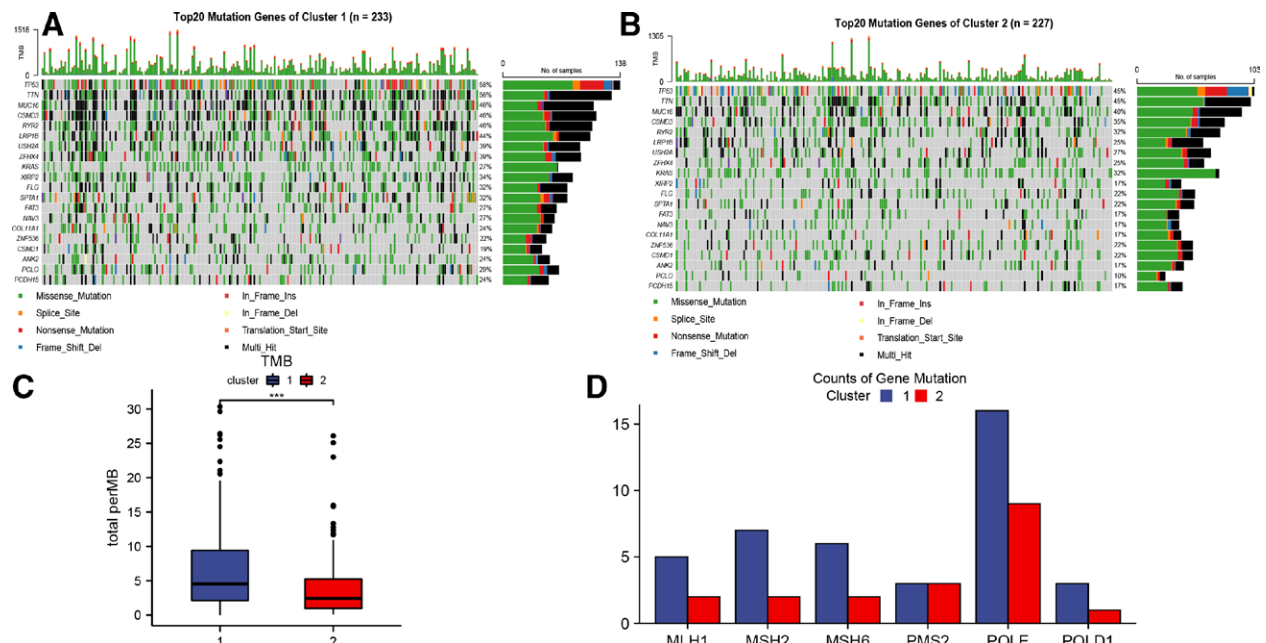


Figure 4. Comparison of mutational landscapes between 2 clusters. Mutational landscape of Cluster 1 (A) and Cluster 2 (B). (C) Comparison of tumor mutation burden (TMB) between 2 clusters. (D) Comparison of gene mutation related to mismatch repair and POLE proofreading domain between 2 clusters. The *P* values are labeled using asterisks (****P* < .001). POLE = polymerase epsilon.

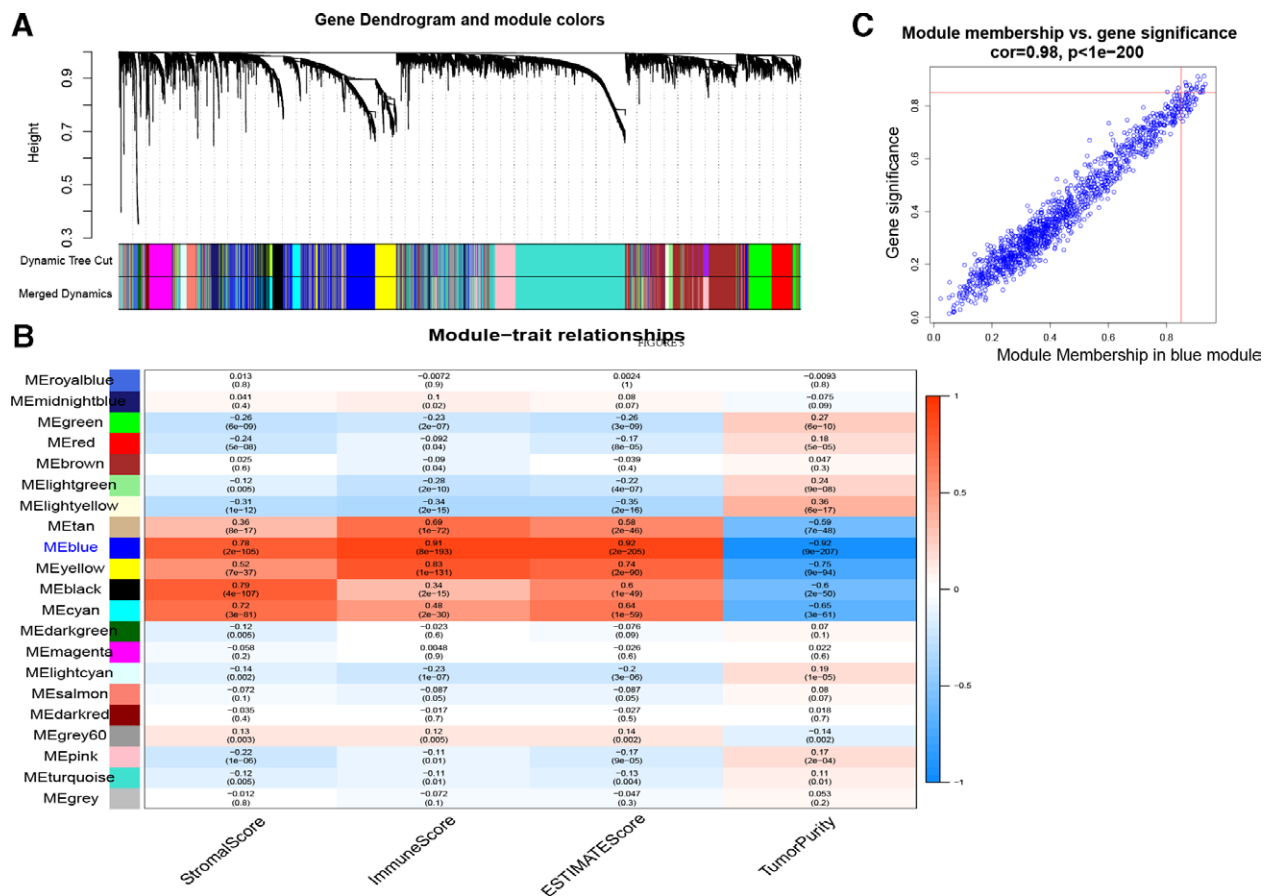


Figure 5. (A) Gene dendrogram and module colors. (B) Heatmap between module eigengenes and ESTIMATE results. (C) Scatterplot of module eigengenes in the blue module.

and D), which again suggests that the effect of immunotherapy may be better in cluster 1.

3.7. Identification of WGCNA with m6a and immune-related hub genes

We obtained 8251 differential genes between the 2 clusters and then subjected the differential genes to WGCNA analysis (Fig. 5A). To identify modules associated with immunity, we performed a correlation analysis between modules and ESTIMATE scores (Fig. 5B). The blue module was chosen because it correlated with immunity ($R = 0.85$, $P = 3e-124$). Thereafter, based on $MM > 0.85$ and $GS > 0.85$ (Fig. 5C), we obtained 22 hub genes from the blue module (CD53, MS4A6A, PLEK, HAVCR2, CYTH4, IL10RA, GIMAP4, CD86, PLEKHO2, LCP2, AIF1, PTPRC, SASH3, LAPTM5, LAIR1, EVI2B, C3AR1, BTK, CYBB, SELPLG, NCKAP1L, CD4).

3.8. Enrichment analysis of hub gene and its correlation with immune infiltration

To determine the biochemical functions of the 22 hub genes, we performed GO enrichment analysis (Fig. 6A). The most important GO term was the positive regulation of T cell proliferation. Protein-protein interaction analysis was also performed (Fig. 6B) and correlations between genes were examined (Fig. 6C). Spearman correlation analysis between genes and immune infiltration (ESTIMATE and ssGSEA) showed that the majority of genes were significantly associated with immunity (Fig. 6D and E).

3.9. Validation of immune features between clusters based on GEO database

The 422 LUAD samples from GSE68465 were divided into 2 clusters according to TCGA (Fig. 7A), and the expression distribution of WTAP and YTHDF2 in both clusters was found to be very similar to that in TCGA. The expression of immunomodulatory targets and the degree of immune infiltration (ESTIMATE, CIBERSORT and ssGSEA) were assessed in the same way (Fig. 7B–H). Cluster 1 was significantly more active than cluster 2 in terms of the immune system.

3.10. Validation of WTAP and YTHDF2 expression levels in LUAD and adjacent tissues

We detected WTAP and YTHDF2 expression levels in 9 LUAD tissues and paired adjacent tissues by real-time quantitative polymerase chain reaction. The results showed that the expression level of WTAP was low in LUAD tissues, while the expression level of YTHDF2 was higher than that of adjacent paired tissues (Fig. 8).

4. Discussion

WTAP is expressed at low levels in LUAD tissues, and it was shown that PCGEM1 can accelerate the progression of NSCLC by inducing miR-433-3p to upregulate WTAP.^[26] This demonstrates that WTAP is a risk factor for lung cancer. YTHDF2 inhibits LUAD cell migration and invasion through regulation of the FAM83D-TGFβ1-pSMAD2/3 pathway, suggesting that YTHDF2 is a lung cancer suppressor.^[27] Although WTAP and YTHDF2 have been shown to correlate with response to

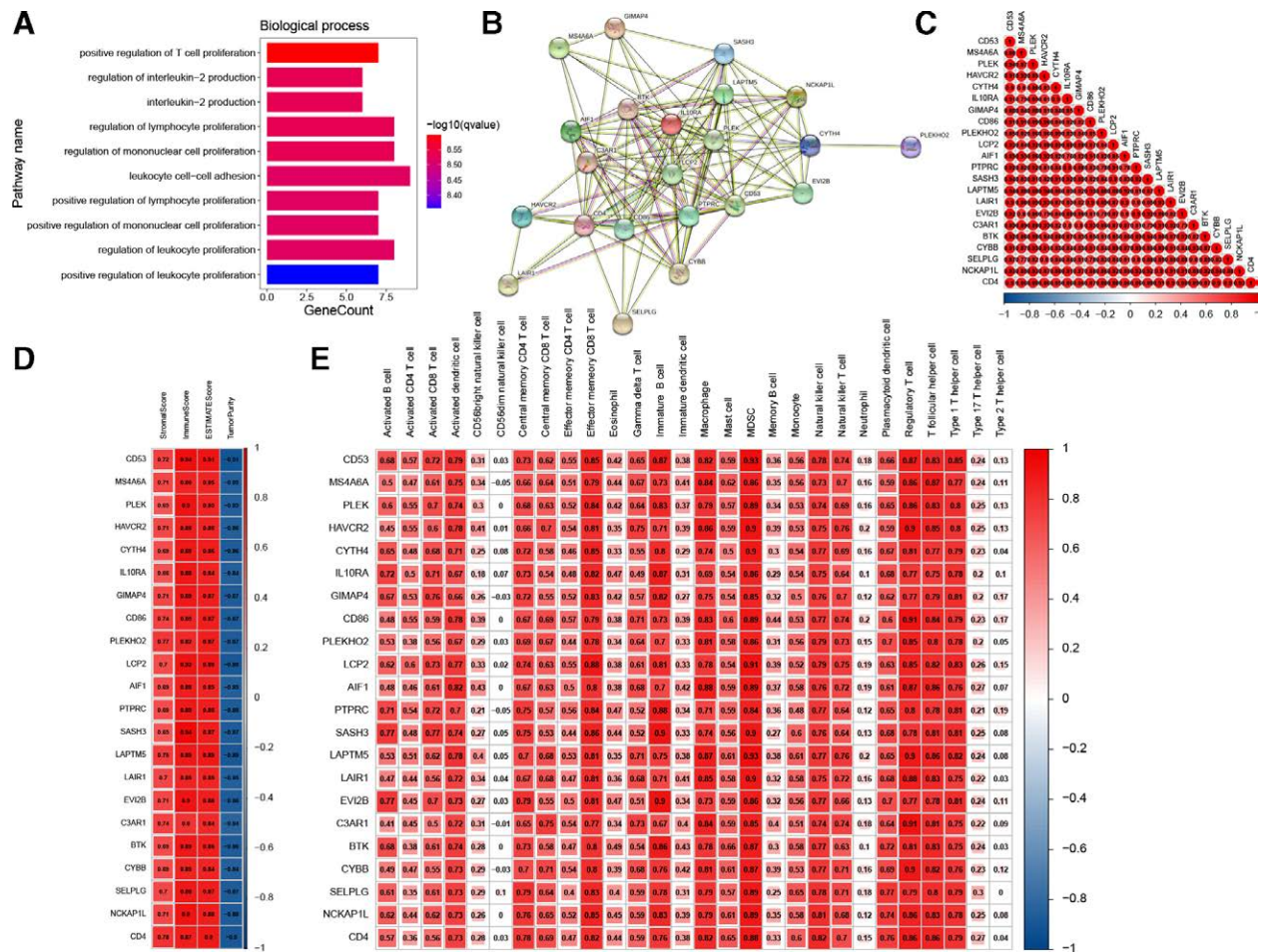


Figure 6. Analysis of 22 hub genes. (A) The GO analysis of hub genes. (B) PPI network of hub genes. (C) Correlation between hub genes. (D) Correlation between hub genes and results of ESTIMATE. (E) Correlation between hub genes and expression of immune cells (ssGSEA). GO = gene ontology, PPI = protein-protein interaction, ssGSEA = single-sample gene set enrichment analysis.

anti-PD1 therapy in hepatocellular carcinoma.^[28] However, the relationship between WTAP and YTHDF2 expression and immunotherapy response in LUAD patients remains to be investigated. In our study, the expression of WTAP and YTHDF2 in LUAD patients was consistent with that in previous studies. In the ESTIMATE analysis, they correlated with immune scores in the opposite way. Thus, both WTAP and YTHDF2 may be involved in the regulation of m6A modification and thus influence immune infiltration and response to immunotherapy in LUAD patients.

We applied consistent clustering TCGA of LUAD patients into 2 groups: Cluster 1 (WTAP: high expression; YTHDF2: low expression) and Cluster 2 (YTHDF2: high expression; WTAP: low expression). To further investigate the functional differences between these 2 clusters, we found that some immune-related pathways (e.g., adaptive immune response, cell chemotaxis, cytokine mediated signaling pathway, cytokine production, humoral immune response, inflammatory response, innate immune response and leukocyte chemotaxis) were enriched in cluster 1 by GSEA. This suggests that cluster 1 may play a more active role in the immune response than cluster 2.

Next, we compared the immune characteristics of these 2 clusters using ESTIMATE, CIBERSORT and ssGSEA methods. In ESTIMATE analysis, cluster 1 was shown to have higher stromal, immune and ESTIMATE scores than cluster 2, thus indicating that cluster 1 has a more active tumor immune micro-environment. In the CIBERSORT analysis, the proportion of CD8 T cells was significantly higher in cluster 1. It was shown

that CD8 T cells are able to significantly influence the prognosis of tumor patients in most tumor-infiltrating immune cell subtypes.^[29] In the ssGSEA analysis, 25 immune cell subtypes showed significantly higher expression in cluster 1, including CD8 T cells, T helper cells (CD4), dendritic cells (DCs), natural killer (NK) cells, natural killer T (NKT) cells, and macrophages. Tumor-infiltrating T cells have a significant impact on the clinical properties of LUAD. High infiltration of CD8 T cells predicts response to drugs,^[30,31] while high CD8 + infiltration is a good prognostic marker for NSCLC.^[32] DCs cells are key antigen-presenting cells that promote antitumor immunity by activating T cells.^[33] NKT cells can reactivate depleted CD8 T cells in anti-PD-1 resistant tumor models and therefore play a key role in antitumor immunotherapy^[34] Macrophages are usually divided into M1 (pro-inflammatory; anti-tumor) and M2 (anti-inflammatory; tumor-promoting) subtypes. According to the results of CIBERSORT analysis, cluster 1 has a higher proportion of M1 subtype macrophages than cluster 2, suggesting that cluster 1 can easily achieve an anti-tumor Th1-type response, while cluster 2 tends to establish a tolerogenic micro-environment.^[35] Based on studies of the immune environment, cluster 1 has a more extensive infiltration of immune cells than cluster 2. Therefore, cluster 1 may have a stronger immune capacity and is more likely to benefit from immunotherapy.

Previous studies reported that programmed cell death 1 (PD1), programmed cell death 1 ligand 1 (PDL1), and cytotoxic T lymphocyte antigen 4 (CTLA4) are approved as targets of ICIs by the FDA.^[36] In addition, lymphocyte activation gene-3

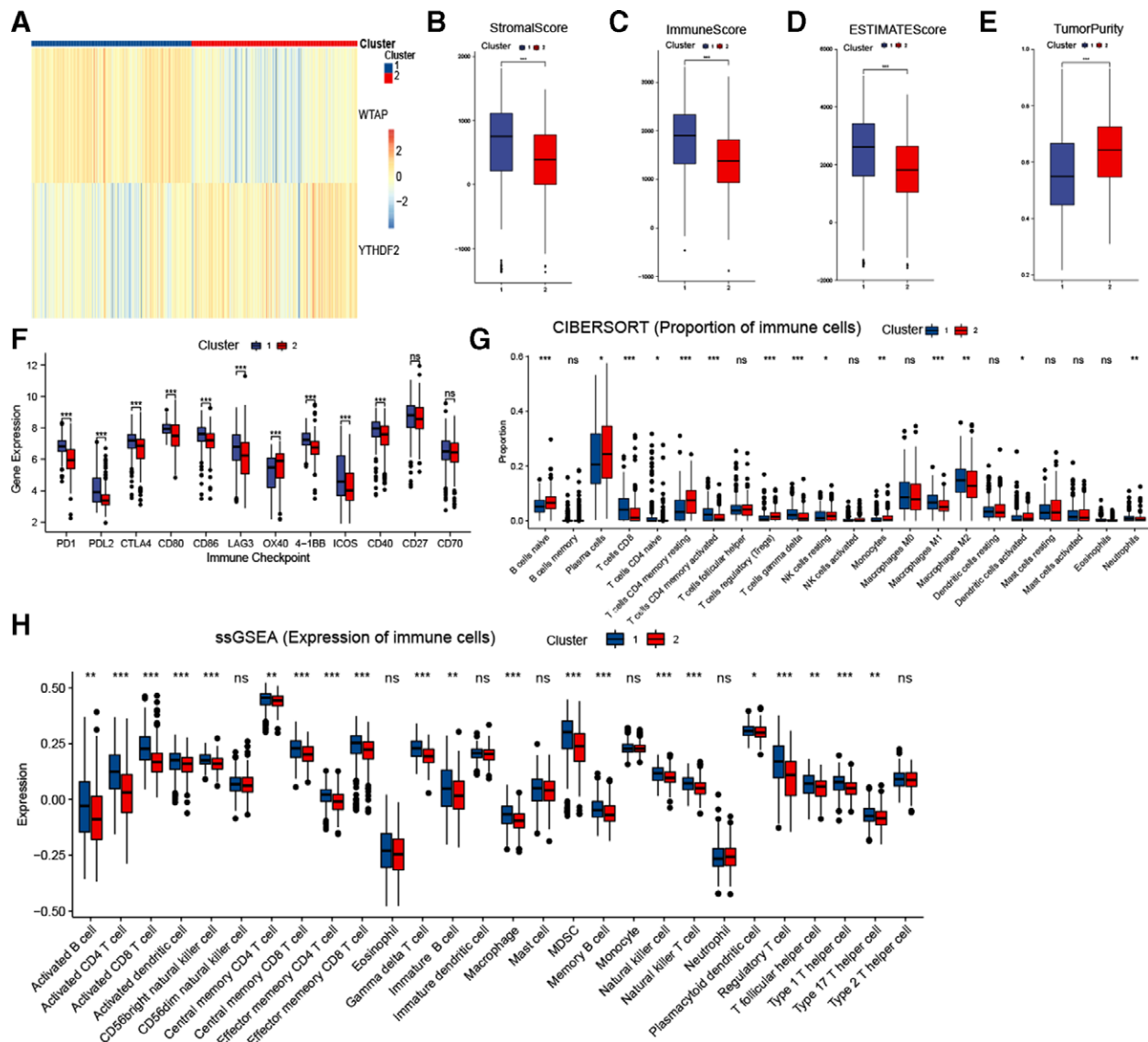


Figure 7. GSE68465 validation of immune contexture between 2 clusters. (A) GSE68465 patients are divided into 2 clusters according to WTAP and YTHDF2. Comparison of stromal score (B), immune score (C), ESTIMATE score (D), tumor purity(E), targets of immunomodulatory drugs (F), proportion of immune cells (G) and expression of immune cells(H) between 2 clusters. The *P* values are labeled using asterisks (ns, no significance, **P* < .05, ***P* < .01, ****P* < .001). GSEA = gene set enrichment analysis, WTAP = N6-methyladenosine (m6A) methyltransferase, YTHDF2 = N6-methyladenosine (m6A) reader proteins.

(LAG3), T cell immunoglobulin-3 (TIM3), and T cell immunoglobulin and ITIM domain (TIGIT) are regarded as co-inhibitory receptor targets.^[37] In this study, we compared 2 clusters of immunomodulatory drugs. In patients with tumors treated with immunotherapy, high PD-1 and CTLA4 levels predicted better survival.^[38] Most of these targets, especially (PD-1, CTLA4), were found to be significantly high in expression in Cluster 1, this suggests that cluster 1 may have a better immunotherapeutic effect.

We analyzed the mutational landscape of the 2 clusters and found significant differences between them. We found that cluster 1 had more TMBs than cluster 2. TMBs may affect the production of immunogenic peptides and thus the response to immunotherapy.^[39] TMB has been shown to be a useful biomarker for ICIs selection in certain cancer types and the expression of TMB and PD-L1 was consistent. High TMB is always beneficial for ICIs treatment.^[40] A study has shown that, in lung cancer, high TMB(TMB-H) tumors exhibited a 39.8% ORR to ICIs (95% CI 34.9–44.8), which was significantly higher than that observed in low TMB (TMB-L) tumors (odds ratio

(OR) = 4.1, 95% CI 2.9–5.8, *P* < 2 × 10⁻¹⁶). Our study showed that cluster 1 had more TMB and expression of PD-L1 than cluster 2, consistent with previous findings. Suggesting that cluster 1 was more likely to benefit from immunotherapy.

Previous studies have shown that MSI-H/dMMR predicts the efficacy of immunotherapy for gastric and colon cancer, and although MSI-H/dMMR is less prevalent in lung cancer,^[41] a trend towards higher survival and response to ICIs was observed in NSCLC dMMR in a recent study.^[42] POLE mutations are NSCLC patients is an uncommon phenotype, and TMB, PD-L1 expression and CD8-positive TIL are higher in mutant patients compared to wild-type POLE, and POLE mutations may represent candidate biomarkers of response to immunotherapy in NSCLC patients.^[43] Our study showed that cluster 1 had higher mutation rates of MMR-related genes (MLH1, MSH2, MSH6, and PMS2) and POLE/POLD1 compared to cluster 2, thus implying that cluster 1 would show a better immunotherapeutic effect.

Next, we used WGCNA to identify 2 blue modules that clustered differentially in WTAP/YTHDF2 and immune scores.

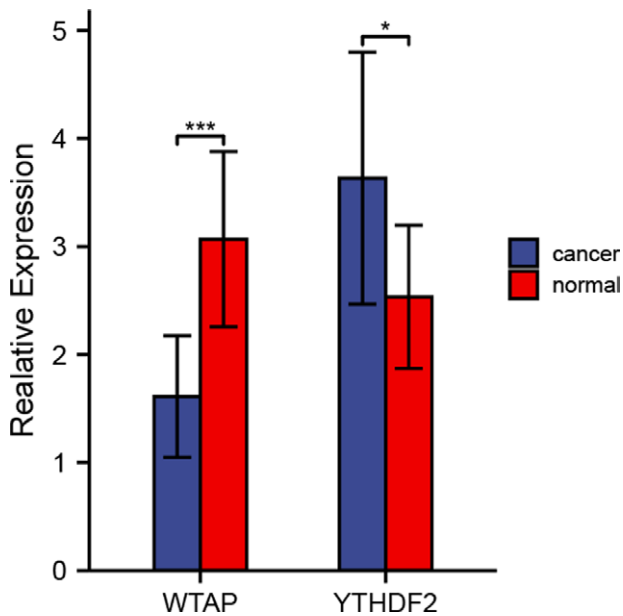


Figure 8. The expression of WTAP and YTHDF2 in LUAD tissues was verified by RT-qPCR. RT-qPCR = Real-time quantitative Polymerase Chain Reaction, WTAP = N6-methyladenosine (m6A) methyltransferase, YTHDF2 = N6-methyladenosine (m6A) reader proteins.

Based on MM and GS, we obtained 22 genes from this module, including TIM3 (HAVCR2) and CD86. By assessing the degree of immune cell infiltration, expression of ICIs and TMB, we hypothesized that cluster 1 could obtain a better immunotherapeutic response than cluster 2; this difference could be caused by WTAP and YTHDF2-mediated m6A modifications.

Based on immunological features, cluster 1 is considered to be a hot tumor, while cluster 2 is more biased towards cold tumors.^[44] WTAP and YTHDF2 may play a potential role in the transition from cold to hot tumors in LUAD. Several studies have shown that targeting dysregulated m6A regulators with small molecule inhibitors has therapeutic potential for cancer treatment. Several biotechnology companies have begun to develop small molecule inhibitors targeting m6A regulators.^[10] In our study, WTAP and YTHDF2 expression were closely related to immune infiltration, ICIs target gene expression and TMB, which makes them potential as drug targets.

Although the combined analysis improved the understanding of the WTAP/YTHDF2-immune relationship and we used 422 GSE68465 patients as an external validation set, the current study still has some limitations. First, this was a retrospective study, and future prospective studies should be conducted in order to avoid bias associated with retrospective studies. Second, the study was based on transcriptomic data from TCGA and GEO, which could not account for WTAP and YTHDF2 expression at the protein level. The most important thing is that our work only proves that the expression levels of WTAP and YTHDF2 in clinical specimens have a certain trend. We cannot conclude the direct mechanism of WTAP and YTHDF2 affecting the immune microenvironment. To overcome these limitations, future detailed molecular and cellular mechanistic studies of WTAP and YTHDF2 and prospective studies including WTAP and YTHDF2 expression, immune cell infiltration and efficacy of immunotherapy in tumor patients will help provide definitive answers.

5. Conclusion

Clustering patients with TCGA-LUAD and GSE68465 by WTAP and YTHDF2 expression, we demonstrated that cluster 1 (WTAP:

high expression; YTHDF2: low expression) had more immune cell infiltration, expression of ICIs targets, and TMB than cluster 2 (WTAP: low expression; YTHDF2: high expression). Thus, suggesting that cluster 1 has a better response to immunotherapy. In conclusion, the expression of WTAP and YTHDF2 is associated with the immune microenvironment of LUAD. These m6A proteins may be novel prognostic and druggable targets associated with the immune system of lung cancer tumors.

Acknowledgments

We acknowledge TCGA and GEO database for providing their platforms, contributors for uploading their meaningful datasets and the Department of Oncology of Weifang Hospital of Traditional Chinese Medicine.

Author contributions

Data curation: Xinyu Zhang.

Funding acquisition: Xinsheng Cai.

Investigation: Xinyu Zhang.

Methodology: Xinyu Zhang.

Software: Xinyu Zhang.

Supervision: Xinsheng Cai.

Validation: Xinyu Zhang.

Visualization: Xinyu Zhang.

Writing – original draft: Xinyu Zhang.

Writing – review & editing: Xinsheng Cai.

References

- [1] Sung H, Ferlay J, Siegel RL, et al. Global Cancer Statistics 2020: GLOBOCAN estimates of incidence and mortality worldwide for 36 cancers in 185 countries. *CA Cancer J Clin.* 2021;71:209–49.
- [2] Ettinger DS, Wood DE, Aggarwal C, et al. NCCN Guidelines insights: non-small cell lung cancer, version 1.2020. *J Natl Compr Canc Netw.* 2019;17:1464–72.
- [3] Miller KD, Nogueira L, Mariotto AB, et al. Cancer treatment and survivorship statistics, 2019. *CA Cancer J Clin.* 2019;69:363–85.
- [4] Siegel RL, Miller KD, Jemal A. Cancer statistics, 2019. *CA Cancer J Clin.* 2019;69:7–34.
- [5] Doroshow DB, Sanmamed MF, Hastings K, et al. Immunotherapy in non-small cell lung cancer: facts and hopes. *Clin Cancer Res.* 2019;25:4592–602.
- [6] Zhou C, Molinier B, Daneshvar K, et al. Genome-wide maps of m6A circRNAs identify widespread and cell-type-specific methylation patterns that are distinct from mRNAs. *Cell Rep.* 2017;20:2262–76.
- [7] Yang D, Qiao J, Wang G, et al. N6-Methyladenosine modification of lincRNA 1281 is critically required for mESC differentiation potential. *Nucleic Acids Res.* 2018;46:3906–20.
- [8] Desrosiers R, Friderici K, Rottman F. Identification of methylated nucleosides in messenger RNA from Novikoff hepatoma cells. *Proc Natl Acad Sci USA.* 1974;71:3971–5.
- [9] Nombela P, Miguel-López B, Blanco S. The role of m6A, m6C and Ψ RNA modifications in cancer: novel therapeutic opportunities. *Mol Cancer.* 2021;20:18.
- [10] Huang H, Weng H, Chen J. m6A modification in coding and non-coding RNAs: roles and therapeutic implications in cancer. *Cancer Cell.* 2020;37:270–88.
- [11] Chen Y, Peng C, Chen J, et al. WTAP facilitates progression of hepatocellular carcinoma via m6A-HuR-dependent epigenetic silencing of ETS1. *Mol Cancer.* 2019;18:127.
- [12] Li H, Su Q, Li B, et al. High expression of WTAP leads to poor prognosis of gastric cancer by influencing tumour-associated T lymphocyte infiltration. *J Cell Mol Med.* 2020;24:4452–65.
- [13] Wang X, Lu Z, Gomez A, et al. N6-methyladenosine-dependent regulation of messenger RNA stability. *Nature.* 2014;505:117–20.
- [14] Ma S, Yan J, Barr T, et al. The RNA m6A reader YTHDF2 controls NK cell antitumor and antiviral immunity. *J Exp Med.* 2021;218:e20210279.
- [15] Tsuchiya K, Yoshimura K, Inoue Y, et al. YTHDF1 and YTHDF2 are associated with better patient survival and an inflamed tumor-immune microenvironment in non-small-cell lung cancer. *Oncoimmunology.* 2021;10:1962656.

- [16] Mayakonda A, Lin D-C, Assenov Y, et al. Maftools: efficient and comprehensive analysis of somatic variants in cancer. *Genome Res.* 2018;28:1747–56.
- [17] Gu Z, Eils R, Schlesner M. Complex heatmaps reveal patterns and correlations in multidimensional genomic data. *Bioinformatics.* 2016;32:2847–9.
- [18] Shedden K, Taylor JMG, Enkemann SA, et al. Gene expression-based survival prediction in lung adenocarcinoma: a multi-site, blinded validation study. *Nat Med.* 2008;14:822–7.
- [19] Yoshihara K, Shahmoradgoli M, Martínez E, et al. Inferring tumour purity and stromal and immune cell admixture from expression data. *Nat Commun.* 2013;4:2612.
- [20] Newman AM, Liu CL, Green MR, et al. Robust enumeration of cell subsets from tissue expression profiles. *Nat Methods.* 2015;12:453–7.
- [21] Hänzelmann S, Castelo R, Guinney J. GSVA: gene set variation analysis for microarray and RNA-seq data. *BMC Bioinf.* 2013;14:7.
- [22] Wilkerson MD, Hayes DN. ConsensusClusterPlus: a class discovery tool with confidence assessments and item tracking. *Bioinformatics.* 2010;26:1572–3.
- [23] Yu G, Wang L-G, Han Y, et al. clusterProfiler: an R package for comparing biological themes among gene clusters. *OMICS.* 2012;16:284–7.
- [24] Love MI, Huber W, Anders S. Moderated estimation of fold change and dispersion for RNA-seq data with DESeq2. *Genome Biol.* 2014;15:550.
- [25] Langfelder P, Horvath S. WGCNA: an R package for weighted correlation network analysis. *BMC Bioinf.* 2008;9:559.
- [26] Weng L, Qiu K, Gao W, et al. LncRNA PCGEM1 accelerates non-small cell lung cancer progression via sponging miR-433-3p to upregulate WTAP. *BMC Pulm Med.* 2020;20:213.
- [27] Zhao T, Wang M, Zhao X, et al. YTHDF2 inhibits the migration and invasion of lung adenocarcinoma by negatively regulating the FAM83D-TGFβ1-SMAD2/3 pathway. *Front Oncol.* 2022;12:763341.
- [28] Jiang H, Ning G, Wang Y, et al. Identification of an m6A-related signature as biomarker for hepatocellular carcinoma prognosis and correlates with sorafenib and anti-PD-1 immunotherapy treatment response. *Dis Markers.* 2021;2021:5576683.
- [29] Bruni D, Angell HK, Galon J. The immune contexture and Immunoscore in cancer prognosis and therapeutic efficacy. *Nat Rev Cancer.* 2020;20:662–80.
- [30] Rizvi NA, Hellmann MD, Snyder A, et al. Cancer immunology. Mutational landscape determines sensitivity to PD-1 blockade in non-small cell lung cancer. *Science.* 2015;348:124–8.
- [31] Munari E, Marconi M, Querzoli G, et al. Impact of PD-L1 and PD-1 expression on the prognostic significance of CD8 tumor-infiltrating lymphocytes in non-small cell lung cancer. *Front Immunol.* 2021;12:680973.
- [32] Rashed HE, Abdelrahman AE, Abdelgawad M, et al. Prognostic significance of programmed cell death ligand 1 (PD-L1), CD8+ tumor-infiltrating lymphocytes and p53 in non-small cell lung cancer: an immunohistochemical study. *Turk Patoloji Derg.* 2017;1:211–22.
- [33] Wculek SK, Cueto FJ, Mujal AM, et al. Dendritic cells in cancer immunology and immunotherapy. *Nat Rev Immunol.* 2020;20:7–24.
- [34] Bae E-A, Seo H, Kim B-S, et al. Activation of NKT Cells in an anti-PD-1-resistant tumor model enhances antitumor immunity by reinvigorating exhausted CD8 T cells. *Cancer Res.* 2018;78:5315–26.
- [35] Aras S, Zaidi MR. TAMEless traitors: macrophages in cancer progression and metastasis. *Br J Cancer.* 2017;117:1583–91.
- [36] Reck M, Remon J, Hellmann MD. First-line immunotherapy for non-small-cell lung cancer. *J Clin Oncol.* 2022;40:586–97.
- [37] Anderson AC, Joller N, Kuchroo VK. Lag-3, Tim-3, and TIGIT: co-inhibitory receptors with specialized functions in immune regulation. *Immunity.* 2016;44:989–1004.
- [38] Liu J-N, Kong X-S, Huang T, et al. Clinical implications of aberrant PD-1 and CTLA4 expression for cancer immunity and prognosis: a pan-cancer study. *Front Immunol.* 2020;11:2048.
- [39] Havel JJ, Chowell D, Chan TA. The evolving landscape of biomarkers for checkpoint inhibitor immunotherapy. *Nat Rev Cancer.* 2019;19:133–50.
- [40] Chan TA, Yarchoan M, Jaffee E, et al. Development of tumor mutation burden as an immunotherapy biomarker: utility for the oncology clinic. *Ann Oncol.* 2019;30:44–56.
- [41] Hause RJ, Pritchard CC, Shendure J, et al. Classification and characterization of microsatellite instability across 18 cancer types. *Nat Med.* 2016;22:1342–50.
- [42] Olivares-Hernández A, Del Barco Morillo E, Parra Pérez C, et al. Influence of DNA Mismatch Repair (MMR) system in survival and response to Immune Checkpoint Inhibitors (ICIs) in Non-Small Cell Lung Cancer (NSCLC): retrospective analysis. *Biomedicines.* 2022;10:360.
- [43] Song Z, Cheng G, Xu C, et al. Clinicopathological characteristics of POLE mutation in patients with non-small-cell lung cancer. *Lung Cancer.* 2018;118:57–61.
- [44] Galon J, Bruni D. Approaches to treat immune hot, altered and cold tumours with combination immunotherapies. *Nat Rev Drug Discov.* 2019;18:197–218.